Eur. Phys. J. C (2016) 76:518
DOI 10.1140/epjc/s10052-016-4360-x

THE EUROPEAN PHYSICAL JOURNAL C

Regular Article - Theoretical Physics

η_c production associated with light hadrons at the B-factories and the future Super B-factories

Qin-Rong Gong[1], **Zhan Sun**[2], **Hong-Fei Zhang**[3,a], **Xue-Mei Mo**[4]

[1] Department of Physics and State Key Laboratory of Nuclear Physics and Technology, Peking University, Beijing 100871, People's Republic of China
[2] School of Science, Guizhou Minzu University, Guiyang 550025, People's Republic of China
[3] School of Science, Chongqing University of Posts and Telecommunications, Chongqing 400065, People's Republic of China
[4] Institute of Digital Medicine, School of Biomedical Engineering, Third Military Medical University, Chongqing 400038, People's Republic of China

Received: 28 June 2016 / Accepted: 7 September 2016 / Published online: 24 September 2016

Abstract We present a complete study of the associated production of the η_c meson with light hadrons in e^+e^- collisions at the B-factory energy, which is demonstrated to be one of the best laboratories for testing the colour-octet (CO) mechanism. The colour-singlet contributions are evaluated up to $O(\alpha^2\alpha_s^3)$, while the CO ones are evaluated up to $O(\alpha^2\alpha_s^2)$. For the first time, the angular distribution of the ${}^1S_0^{[8]}$ production is studied at QCD next-to-leading order. We find that the ${}^1S_0^{[8]}$ channel dominates the total cross section, while the ${}^1P_1^{[8]}$ one exhibits its importance in the angular distribution, which turns out to be downward going with respect to $\cos\theta$. This can be considered as the most distinct signal for the CO mechanism.

1 Introduction

η_c (0^{-+}), known as the lightest charmonium state, can provide a very good laboratory for the study of the quarkonium production mechanism. However, in contrast to the copious data on the J/ψ yield, the observation of the η_c meson is scant. This is basically because the J/ψ can be detected via its leptonic decay channels, while the fragments of the η_c decays are dominated by multiple hadrons [1], both the observation and the reconstruction of which are more difficult. A novel approach to the measurement of the various charmonium states using their common decay channel to $p\bar{p}$ was proposed in Ref. [2], which shed light on the investigation of the η_c and h_c mesons. By exploiting this approach, the LHCb Collaboration [3] achieved their first study of the inclusive and prompt η_c yield in pp collisions. They found that the η_c hadroproduction cross section is even larger than that of the J/ψ in the same experimental condition. On the theory side, QCD leading order (LO) calculation of the η_c hadroproduction within the nonrelativistic QCD (NRQCD) [4] was accomplished in Refs. [5,6], following which the complete QCD next-to-leading order (NLO) studies came out in a few weeks [7–9]. Ref. [7] considered the LHCb data on η_c hadroproduction as the challenge to NRQCD, while Refs. [8,9] found these data did not bring about any inconsistency. Reference [9] further argued that this measurement actually provided an excellent opportunity for fixing the η_c (as well as the J/ψ) wave function at the origin, and can also help with the determination of the colour-octet (CO) long-distance matrix elements (LDMEs) for the J/ψ production. As was pointed out in Ref. [10], only two degrees of freedom of the three J/ψ CO LDMEs can be fixed by the J/ψ yield data. η_c data helped to fix the last one, $\langle O^{J/\psi}({}^1S_0^{[8]})\rangle$. Having this parameter fixed, Ref. [11] discovered some interesting features of the J/ψ hadroproduction and polarisation, which provided a possibility for the solution to the long-standing J/ψ polarisation puzzle.

In fact, as early as 17 years ago, η_c photo- and leptoproduction as a heuristic probe to the CO mechanism has already been proposed [12,13]. In these processes, the colour-singlet (CS) channel is suppressed by an order of α_s^2 compared to the ${}^1S_0^{[8]}$ channel, which, on the one hand, provided an opportunity to test the CO mechanism, on the other hand, could help to fix the ${}^1S_0^{[8]}$ LDME for η_c production. Unfortunately, due to lack of data, this device has never been put into implementation.

Similar to the η_c photo- and leptoproduction, η_c production in e^+e^- annihilation also shows these good features. This process becomes more important since the B-factories increased their luminosity to the order of 10^{34} cm^{-2} s^{-1} (10^{-2} pb^{-1} s^{-1}). Two Super B-factories [14,15] are pro-

[a] e-mail: hfzhang@ihep.ac.cn

posed to reach even higher luminosities, on the order of 10^{36} cm^{-2} s^{-1} (1 pb^{-1} s^{-1}). A few years running of these machines can accumulate adequate data for a precision measurement of the η_c production, which, as will be shown later, may provide the most distinct test of NRQCD.

For the η_c production, up to v^4, one CS state ($^1S_0^{[1]}$) and three CO states ($^1S_0^{[8]}$, $^3S_1^{[8]}$ and $^1P_1^{[8]}$) are involved. At the B-factory energy, charge parity is approximately conserved. The CS state can only be produced with at least three gluons emitted. This process is of order $\alpha^2\alpha_s^3$. However, $^1S_0^{[8]}$ state can be produced with only one gluon emitted, which is of order $\alpha^2\alpha_s$, two orders lower than the CS one in α_s. We can expect the CO processes be more significant than the CS one. Thus the measurement can definitely distinguish the two mechanisms.

Another interesting feature of this process is that, in contrast to the η_c hadroproduction case in which the $^3S_1^{[8]}$ channel dominates the production, η_c production in e^+e^- annihilation is dominated by the $^1S_0^{[8]}$ and $^1P_1^{[8]}$ channels. The LDMEs for these channels are related to the $^3S_1^{[8]}$ and $^3P_J^{[8]}$ LDMEs for the J/ψ production by the heavy quark spin symmetry (HQSS). Since the determination of the J/ψ LDMEs is still facing controversy [7–9,16–21], this process may help to clarify this issue.

The last but not the least important thing to mention: the measurement of the η_c production at B-factories might provide some useful information for the study of the process $e^+e^- \to J/\psi + X$, which was measured by the BABAR [22] and Belle [23–25] Collaborations. The theoretical studies of these experiments are presented in Refs. [16,26–35], which found that the CS results of the total cross sections generally saturate the most recent Belle measurement [25], and the inclusion of the CO contributions would ruin the agreement between theory and experiment. In spite of this, the angular distribution [31], within the CS mechanism, for the production of the J/ψ in association with either light hadrons or charmed hadrons is in conflict with the data given in the same experimental paper. Reference [9] suggested that the CS LDME for the J/ψ production might be smaller than the ordinarily used values obtained in potential-model calculations [36], which left room for the CO mechanism. The smaller CS LDME and the inclusion of the CO contributions can provide opportunities for the understanding of the angular distribution puzzle. However, the results given by employing the LDMEs in Ref. [9] exceed the Belle measurement of the production of the J/ψ plus light hadrons. This problem is still waiting for further investigation. Actually, many factors can cause this discrepancy. For example, the α_s^2 corrections are always significant [37–39], thus the universality of the LDMEs at QCD NLO cannot take the responsibility of testing NRQCD. Before we can achieve the high-order calculations, η_c production at B-factories can serve as an alternative test of the CO mechanism. Since this process is dominated by the $^1S_0^{[8]}$ and $^1P_1^{[8]}$ channels, the measurement can, on the one hand, distinguish the CS and CO contributions, on the other hand, specify whether the theoretical results for the $c\bar{c}(^1S_0^{[8]})$ production in e^+e^- annihilation reach a good convergence up to QCD NLO.

In this paper, we study the η_c associated production with light hadrons at B-factory energy within the NRQCD framework, which can provide references for the future experiment at the Super B-factories. The rest of this paper is organised as follows. In Sect. 2, we briefly describe the framework of our calculation. Section 3 presents the numerical results and discussions, while we come to our conclusions in Sect. 4.

2 η_c associated production with light hadrons within the NRQCD framework

In the NRQCD factorisation framework, up to v^4, four intermediate $c\bar{c}$ states, including one CS state ($^1S_0^{[1]}$) and three CO states ($^1S_0^{[8]}$, $^3S_1^{[8]}$ and $^1P_1^{[8]}$), are involved in the η_c production. The cross section for the direct η_c production in association with light hadrons in e^+e^- collisions can thus be expressed as

$$\begin{aligned} &\mathrm{d}\sigma(e^+e^- \to \eta_c + X) \\ &= \sum_n \mathrm{d}\hat{\sigma}(e^+e^- \to c\bar{c}(n) + X)\langle O^{\eta_c}(n)\rangle, \end{aligned} \tag{1}$$

where n runs over the four intermediate states, $\hat{\sigma}$ are the corresponding short-distance coefficients (SDCs), and X denotes light hadrons, the hadronisation process of which are not concerned in our calculation. Thus, we simply evaluate the processes in which X are partons (gluons and/or light quarks).

The charge parity of the CS state, $^1S_0^{[1]}$, is $+1$. Since the charge parity is conserved in strong and electromagnetic interactions, this state can be produced with at least three gluons emitted. However, the LO processes for $^1S_0^{[8]}$, $^3S_1^{[8]}$ and $^1P_1^{[8]}$ productions involve only one, two and two emitted gluons, respectively. This results in the fact that the CS contributions are greatly suppressed compared with the CO one. In this paper, we consider the CS contribution at LO ($\alpha^2\alpha_s^3$). There is only one process at this order, namely

$$e^+e^- \to c\bar{c}(^1S_0^{[1]}) + g + g + g, \tag{2}$$

where g denotes a gluon.

The CO processes are evaluated up to the order $\alpha^2\alpha_s^2$, which is, for both the $^3S_1^{[8]}$ and the $^1P_1^{[8]}$ channels, LO, while for the $^1S_0^{[8]}$ channel, NLO in α_s. The processes involved are

$$e^+e^- \to c\bar{c}(^1S_0^{[8]}) + g, \tag{3}$$

$$V : e^+e^- \to c\bar{c}(^1S_0^{[8]}) + g, \tag{4}$$

$$e^+e^- \to c\bar{c}(^1S_0^{[8]}) + g + g, \tag{5}$$
$$e^+e^- \to c\bar{c}(^1S_0^{[8]}) + q + \bar{q}, \tag{6}$$
$$e^+e^- \to c\bar{c}(^3S_1^{[8]}) + g + g, \tag{7}$$
$$e^+e^- \to c\bar{c}(^3S_1^{[8]}) + q + \bar{q} \tag{8}$$
$$e^+e^- \to c\bar{c}(^1P_1^{[8]}) + g + g, \tag{9}$$

where q and $\bar{q}$ represent light quark and antiquark, respectively, and the label V means one-loop-level virtual correction to the process on the right-hand side of it. Summing over the processes in Eqs. (4), (5) and (6), the cross section for the η_c production via the $^1S_0^{[8]}$ channel at QCD NLO will be free from a divergence, while those for the processes listed in Eqs. (2), (3), (7) and (8) are nonsingular in themselves. However, the process in Eq. (9) is divergent. This divergence can be cancelled within the NRQCD framework by including the QCD corrections to the $^1S_0^{[8]}$ LDME. Summing the two contributions stated above, we can redefine the $^1P_1^{[8]}$ SDC as a finite quantity. The detail of this procedure can be found in Refs. [40–42], so, we just omit these discussions in the current paper, and purloin the useful equations in the references. One important feature necessary for our discussion is that the SDC for the $^1P_1^{[8]}$ channel can be decomposed in two parts,

$$\hat{\sigma}(e^+e^- \to c\bar{c}(^1P_1^{[8]}) + g + g) = \hat{\sigma}_{\rm foml} - \frac{\alpha_s}{9\pi m_c^2}\frac{N_c^2-4}{N_c}\ln\left(\frac{\mu_\Lambda^2}{m_c^2}\right)\hat{\sigma}(e^+e^- \to c\bar{c}(^1S_0^{[8]}) + g), \tag{10}$$

where $\hat{\sigma}_{\rm foml}$ is completely free from μ_Λ, the NRQCD factorisation scale.

Then we rewrite Eq. (1), up to the order we maintain in our calculation, in an explicit form as

$$\begin{aligned} {\rm d}\sigma(\eta_c) = {} & {\rm d}\hat{\sigma}(^1S_0^{[1]})\langle O^{\eta_c}(^1S_0^{[1]})\rangle \\ & + {\rm d}\hat{\sigma}(^3S_1^{[8]})\langle O^{\eta_c}(^3S_1^{[8]})\rangle + {\rm d}\hat{\sigma}_{\rm foml}\langle O^{\eta_c}(^1P_1^{[8]})\rangle \\ & - \frac{\alpha_s}{9\pi m_c^2}\frac{N_c^2-4}{N_c}\ln\left(\frac{\mu_\Lambda^2}{m_c^2}\right){\rm d}\hat{\sigma}_{\rm lo}(^1S_0^{[8]})\langle O^{\eta_c}(^1P_1^{[8]})\rangle \\ & + {\rm d}\hat{\sigma}(^1S_0^{[8]})\langle O^{\eta_c}(^1S_0^{[8]})\rangle, \end{aligned} \tag{11}$$

where we have abbreviated the SDCs $\hat{\sigma}(e^+e^- \to n + X)$ as $\hat{\sigma}(n)$. The subscript lo is used to distinguish the QCD LO SDC from the one up to the order of $\alpha^2\alpha_s^2$.

In addition to the direct η_c production, we also consider the feed down contributions from the J/ψ and h_c. For the J/ψ production in e^+e^- annihilation, we employ the Belle data in Ref. [25], in which the cross sections for the J/ψ production in association with light hadrons at the B-factories are obtained to be 0.43 pb. Multiplying the branching ratio from J/ψ to η_c, $\mathcal{B}(J/\psi \to \eta_c) \approx 0.017$ [1], we immediately get the η_c production cross section from the J/ψ as 0.007 pb, which is much smaller than the direct one and can be neglected. However, the h_c feed down contributions are not negligible. This process has been studied in Ref. [40], thus we just employ the results therein.

3 Numerical results and discussions

Having generated all the needed FORTRAN source using the FDC system [43], we start to perform the numerical calculation. The global choice of the parameters is listed as follows: The QED and QCD coupling constants are $\alpha = 1/137$ and $\alpha_s(3\ {\rm GeV}) = 0.26$, respectively. The branching ratio $\mathcal{B}(h_c \to \eta_c) \approx 0.51$ [1]. The colliding energy is fixed at 10.6 GeV, which corresponds to the B-factory and Super B-factory experiments. At this energy, the diagrams involving a Z-boson propagator are greatly suppressed. Therefore we only consider the diagrams in which the electron and the positron annihilate into a virtual photon. We employ the LDMEs for the η_c production obtained in Ref. [9,11,42] as our default choice. The values of them are also presented now:

$$\begin{aligned} &\langle O^{\eta_c}(^1S_0^{[1]})\rangle = (0.215 \pm 0.135)\ {\rm GeV}^3, \\ &\langle O^{\eta_c}(^3S_1^{[8]})\rangle = (0.78 \pm 0.34) \times 10^{-2}\ {\rm GeV}^3, \\ &\langle O^{\eta_c}(^1S_0^{[8]})\rangle \approx \frac{1}{3}\langle O^{J/\psi}(^3S_1^{[8]})\rangle = 0.35 \times 10^{-2}\ {\rm GeV}^3, \\ &\langle O^{\eta_c}(^1P_1^{[8]})\rangle \approx 3\langle O^{J/\psi}(^3P_0^{[8]})\rangle = 5.8 \times 10^{-2}\ {\rm GeV}^3. \end{aligned} \tag{12}$$

The last equation has implicated a redefinition of the P-wave LDMEs by the following equation:

$$\langle O^H(^{2S+1}P_J^{[n]})\rangle = \langle O^H(^{2S+1}P_J^{[n]})\rangle_{\rm BBL}/m_c^2, \tag{13}$$

where we use the subscript "BBL" to denote the definition in Ref. [4]. Our P-wave SDCs are also redefined by multiplying m_c^2 accordingly. The LDMEs for the h_c production are taken from Refs. [36,42] as

$$\begin{aligned} &\langle O^{h_c}(^1P_1^{[1]})\rangle = \frac{27}{2\pi m_c^2}|R'_{h_c}(0)|^2 = 0.143\ {\rm GeV}^3, \\ &\langle O^{h_c}(^1S_0^{[8]})\rangle = 3\langle O^{\chi_{c0}}(^3S_1^{[8]})\rangle \\ &\qquad\qquad = (6.27 \pm 0.12) \times 10^{-3}\ {\rm GeV}^3. \end{aligned} \tag{14}$$

3.1 Total cross sections

In the following discussions, we use $\sigma(n)$ to abbreviate the contribution of the channel n to the cross section up to the order we keep in our calculation. For the $^1S_0^{[8]}$ channel, we are also interested in the significance of the QCD corrections, thus we assign the LO results a distinct name, $\sigma_{\rm lo}(^1S_0^{[8]})$.

Then we can obtain the total cross sections for each channel, while we choose $m_c = 1.5$ GeV, $\mu_r = 2m_c$ as a default input. Although the uncertainties of the LDMEs for $^1S_0^{[1]}$

Table 1 The total cross section for the process $e^+e^- \to \eta_c$+light hadrons. The results contributed by each channel are also presented

n	$^1S_0^{[1]}$	$^1S_0^{[8]}$(LO)	$^1S_0^{[8]}$	$^3S_1^{[8]}$	$^1P_1^{[8]}$	CO	direct	$^1S_0^{[8]}(h_c)$	$^1P_1^{[1]}$	total
$\sigma(n)$(pb)	0.0021	0.043	0.080	0.0128	−0.0032	0.090	0.092	0.073	−0.003	0.162

Table 2 The cross section for the direct process $e^+e^- \to \eta_c$+light hadrons. The results contributed by each channel are also presented

n	$^1S_0^{[1]}$	$^1S_0^{[8]}$(LO)	$^1S_0^{[8]}$	$^3S_1^{[8]}$	$^1P_1^{[8]}$	CO
Butenchon, Kinel [16]	0.0043	0.0066	0.0122	0.0499	0.0007	0.0628
Chao, Ma, Shao, Wang, Zhang [17]	0.0038	0.0123	0.0229	0.1461	−0.0009	0.1681
Gong, Wan, Wang, Zhang [18]	0.0038	−0.0188	−0.0350	0.1592	0.0016	0.1258
Bodwin, Chung, Kim, Lee, Ma [21]	0.0043	−0.0292	−0.0543	0.1805	0.0005	0.1267

and $^3S_1^{[8]}$ are huge, the SDCs for the two channels are so small that these contributions are almost negligible, so, we do not count these uncertainties and just adopt the central value of them. For the h_c feed down contribution, the uncertainty of $\langle O^{h_c}(^1S_0^{[8]})\rangle$ is very small, so we also neglect it in the presentation of the cross sections. The results are listed in Table 1. One can easily find that the CS contribution, although enhanced by the LDME, is almost 50 times smaller than the CO one. This is quite different from the J/ψ case, in which both the CS and the CO contributions are significant. Accordingly, this process can serve as a good laboratory to test NRQCD. Another interesting feature of this process is that the $^1S_0^{[8]}$ channel dominates the total cross section (for both the direct and the feed down part), while the other channels are almost one order of magnitude smaller. Despite the exploration of numerous processes, we have not found an example as clean as this one, for the determination of the LDME $\langle O^{\eta_c}(^1S_0^{[8]})\rangle$.

In addition to the set of the LDMEs employed here, we notice that there are also some other sets, which are presented in Refs. [16–18,21]. In order to study the uncertainties brought about by the LDMEs, we present the results obtained by using them in Table 2. Although each of the sets of the LDMEs completely differs from the other ones, the fact does not change that the CO contribution is more than one order of magnitude larger than the CS one. However, all the other four results are dominated by the $^3S_1^{[8]}$ channel. In the following section, we will see that the cosθ behaviours of the $^3S_1^{[8]}$ channel and the combination of the $^1S_0^{[8]}$ and $^1P_1^{[8]}$ channels are quite different, thus, this difference can distinguish the different sets of the LDMEs.

We also need to study the μ_r and m_c dependence of the total cross section, which implicates the convergence of the perturbative expansion at a fixed order. Before we present the numerical results, we need to address the dependence of the LDMEs on the scales. As Ref. [42] pointed out, the LDMEs do not depend on μ_r, which is a direct conclusion of the equation

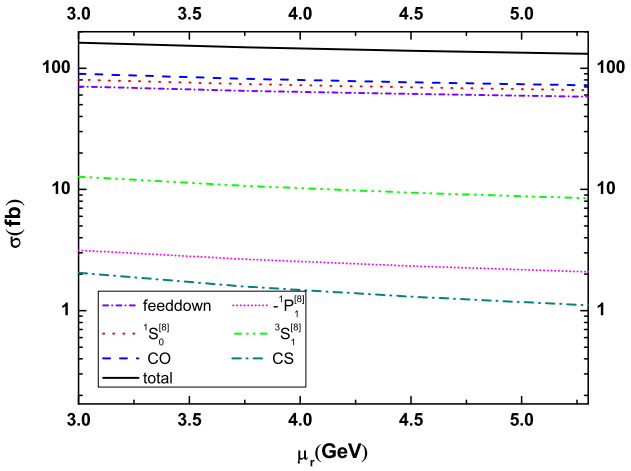

Fig. 1 The μ_r dependence of the total cross sections for the process $e^+e^- \to \eta_c$+ light hadrons

$$\frac{\partial\langle O^H(n)\rangle}{\partial\mu_r} = 0. \tag{15}$$

However, as m_c varies its value, the LDMEs scale as [4,44]

$$\langle O^{\eta_c}(n)\rangle \propto m_c^3. \tag{16}$$

Note that we have redefined the P-wave LDMEs in Eq. (13). Since all the LDMEs we used in this paper are obtained at a fixed value of m_c, we need to take the scaling in Eq. (16) into account in our numerical study.

The μ_r dependence of the total cross sections is presented in Fig. 1, where $m_c = 1.5$ GeV is fixed. One can observe that as μ_r varies from $2m_c = 3$ GeV to $\sqrt{s}/2 = 5.3$ GeV, the total cross section slopes down from 162 to 130 fb, and the CS contribution decreases from 2 to about 1.3 fb. This dependence is comparable with the process $e^+e^- \to J/\psi + X$ [29–31].

In Fig. 2, we present the m_c dependence of the total cross sections, where $\mu_r = 3.0$ GeV is fixed and the scaling in Eq. (16) has been taken into account. Apparently, the m_c

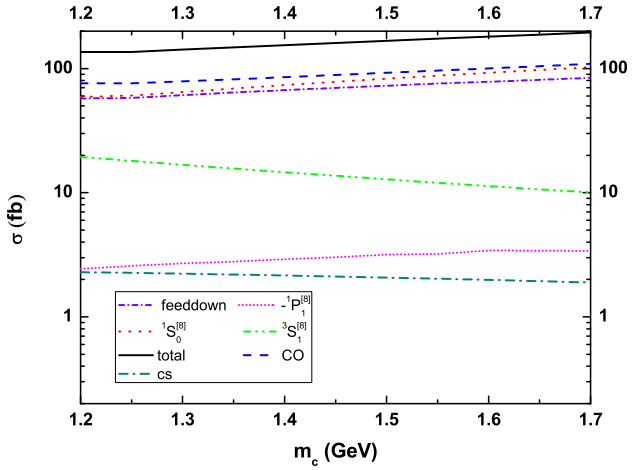

Fig. 2 The m_c dependence of the total cross sections for the process $e^+e^- \to \eta_c+$ light hadrons, where the scaling in Eq. (16) are taken into account

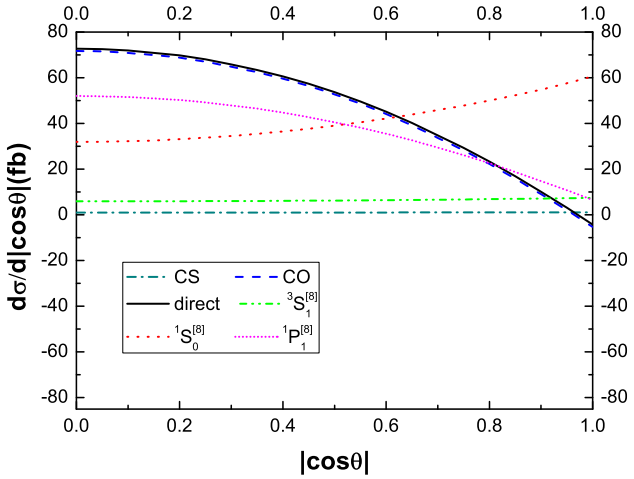

Fig. 3 The differential cross sections for the η_c direct production in the process $e^+e^- \to \eta_c+$ light hadrons with respect to cosθ

dependence for the process we study in this paper is even milder than that for the J/ψ production processes studied in Refs. [29–31].

These results suggest it is reliable that the η_c production in association with light hadrons at B-factories is dominated by the ${}^1S_0^{[8]}$ channel. Accordingly, this experiment can provide an excellent opportunity for the test of the CO mechanism.

3.2 Angular distribution

We present the angular distribution of the η_c production at B-factories in Fig. 3. It is also the first time the angular distribution of the $c\bar{c}({}^1S_0^{[8]})$ state production in e^+e^- annihilation at QCD NLO is given. We recall that the angular distribution for the CS contribution to the process $e^+e^- \to J/\psi + gg$ given in Ref. [31] is flat, while the Belle data [25] goes upward as cosθ increases. Interestingly, the ${}^1S_0^{[8]}$ channel,

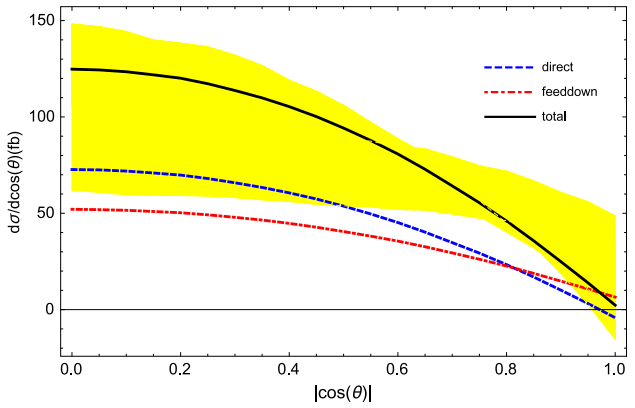

Fig. 4 The differential cross sections for the process $e^+e^- \to \eta_c+$ light hadrons with respect to cosθ

which also contributes to the J/ψ production, has the same cosθ behaviour as the Belle data. This might indicate the existence of the CO contributions in the J/ψ production process at B-factories.

According to Fig. 3, the cosθ distribution is also dominated by the CO channels. However, the ${}^1P_1^{[8]}$ contribution is, yet, not negligible; it completely changes the behaviour of the differential cross section, even though after integrating out cosθ it turns out to be almost zero. The differential cross section with respect to cosθ within the NRQCD framework is downward going. This kind of behaviour can be regarded as the most distinct signal for the CO mechanism.

One might notice the differential cross section turns out to be negative near the point cos$\theta = 1$. This is not such a severe problem as it seems to be. First of all, up to QCD NLO, the terms we keep in the perturbative expansion is NOT a perfect square; the inclusion of the higher-order terms can make the results positive. Alternatively, one can tune the scales to achieve better results. Actually, these two operations have the same basis, since the uncertainty brought about by the different choices of the scales is anyway a higher-order effect.

To investigate whether the feed down contributions from h_c ruin the cosθ behaviour, we present the angular distribution of both the η_c direct production and from the h_c feed down in Fig. 4, from which one can see that the feed down part behaves the same as the direct part. In this figure, we employed different choices of μ_r and m_c and studied the uncertainties brought about by the variation of the two parameters. The band covers the range 1.2 GeV $< m_c <$ 1.7 GeV and 3.0 GeV $< \mu_r <$ 5.3 GeV.

As is mentioned in the previous section, the total cross sections as well as the dominant channels can be quite different if we employ different sets of the LDMEs. This is also true for the angular distribution curves. Since not all the groups provided the CO LDME for the χ_c production, here we only present the angular distribution for the direct

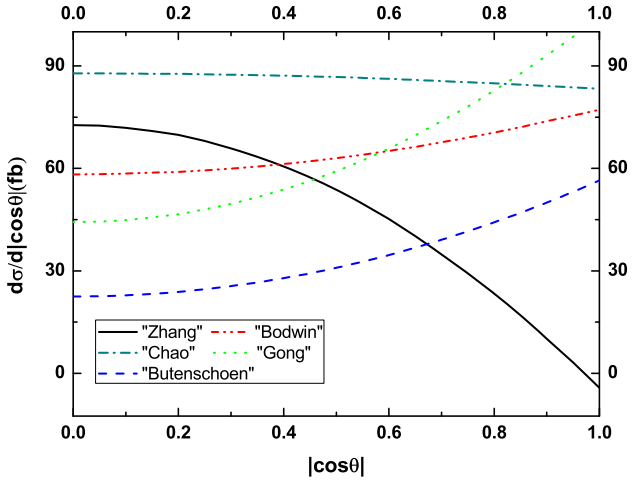

Fig. 5 The differential cross sections for the η_c direct production in the process $e^+e^- \to \eta_c +$ light hadrons with respect to $\cos\theta$. The different curves correspond to different choices of the LDMEs. The labels "Zhang", "Butenschoen", "Chao", "Gong", and "Bodwin" represent employing LDMEs taken from Refs. [9,11], Refs. [16–18], and [21]

η_c production using different sets of the LDMEs provided in Refs. [9,11,16–18,21] in Fig. 5. Apparently, the curves for all the other sets of the LDMEs have different behaviour from our default results. Using the LDMEs presented in Refs. [17,18,21], the curves are upward going, while employing the LDMEs in Ref. [16], the curve is almost flat, with respect to $\cos\theta$. Therefore, this process can distinguish these LDMEs.

3.3 μ_Λ dependence

To study the convergence of the perturbative expansion, we also need to observe the μ_Λ dependence of the cross sections. Here we focus on two questions. (1) Does a different choice of μ_Λ change the behavior of the angular distribution? (2) Does the differential cross section near the point $\cos\theta = 1$ always lie below 0?

As is indicated by Eq. (11), μ_Λ independence requires

$$\mathrm{d}\hat{\sigma}({}^1S_0^{[8]}) \propto \alpha_s \mathrm{d}\hat{\sigma}_{\mathrm{lo}}({}^1S_0^{[8]}) \tag{17}$$

at any value of $\cos\theta$. In this case, when the value of μ_Λ varies, one can preserve the differential cross section results by tuning the value of $\langle O^{\eta_c}({}^1S_0^{[8]})\rangle$.

Here we define

$$r = \frac{\mathrm{d}\hat{\sigma}({}^1S_0^{[8]})}{\alpha_s \mathrm{d}\hat{\sigma}_{\mathrm{lo}}({}^1S_0^{[8]})}, \tag{18}$$

which is slightly different from the definition provided in Ref. [41,42]. If r is a constant with respect to $\cos\theta$, when μ_Λ is changed into μ'_Λ, to make the cross section invariant, the ${}^1S_0^{[8]}$ LDME should be

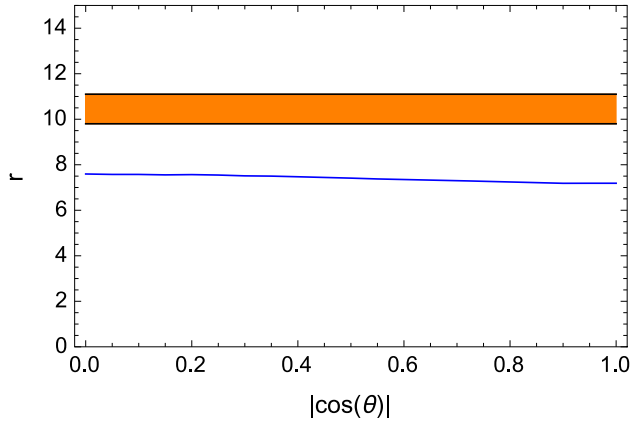

Fig. 6 The value of r defined in Eq. (18) as a function of $\cos\theta$. The *shaded area* correspond to range of r_J obtained in Ref. [42]

$$\langle O^{\eta_c}({}^1S_0^{[8]})\rangle \to \langle O^{\eta_c}({}^1S_0^{[8]})\rangle + \frac{1}{9\pi m_c^2 r}\frac{N_c^2-4}{N_c}\ln\left(\frac{\mu'^2_\Lambda}{\mu^2_\Lambda}\right) \langle O^{\eta_c}({}^1P_1^{[8]})\rangle. \tag{19}$$

This is also consistent with the renormalisation group equation

$$\mu_\Lambda \frac{\partial\langle O^{\eta_c}({}^1S_0^{[8]})\rangle}{\partial\mu_\Lambda} = \frac{2\alpha_s}{9\pi m_c^2}\frac{N_c^2-4}{N_c}\langle O^{\eta_c}({}^1P_1^{[8]})\rangle, \tag{20}$$

once the perturbative expansion reaches good convergence at LO. In this case, r is approximately $1/\alpha_s$.

However, the LDMEs are obtained through the fit of the J/ψ data. If we denote the value of r for the $c\bar{c}({}^3S_1^{[8]})$ hadroproduction as r_J, namely

$$r_J = \frac{\mathrm{d}\hat{\sigma}({}^3S_1^{[8]})}{\alpha_s \mathrm{d}\hat{\sigma}_{\mathrm{lo}}({}^3S_1^{[8]})}, \tag{21}$$

the LDMEs for the J/ψ production also satisfy Eq. (19) once replacing r by r_J:

$$\langle O^{J/\psi}({}^3S_1^{[8]})\rangle \to \langle O^{J/\psi}({}^3S_1^{[8]})\rangle + \frac{1}{\pi m_c^2 r_J}\frac{N_c^2-4}{N_c}\ln\left(\frac{\mu'^2_\Lambda}{\mu^2_\Lambda}\right) \langle O^{\eta_c}({}^3P_0^{[8]})\rangle, \tag{22}$$

where there is multiplication by a factor of 9 to compensate for the difference between the LDME for J/ψ and η_c. Note that $\hat{\sigma}$ in Eq. (21) represents the SDC for the hadroproduction of the corresponding intermediate state. The value of r_J ranges from 9.8 to 11.1, as is obtained in Ref. [42]. In Fig. 6, we can see that the value of r is quite below that of r_J (the shaded area). We adopt the central value of r_J, namely $r_J = 10.5$, and employ Eq. (22) to obtain the LDMEs at different values of μ_Λ. Even though r is almost a constant with respect to $\cos\theta$, having $r \neq r_J$, the cross sections for the process we study in this paper still depend on μ_Λ. To

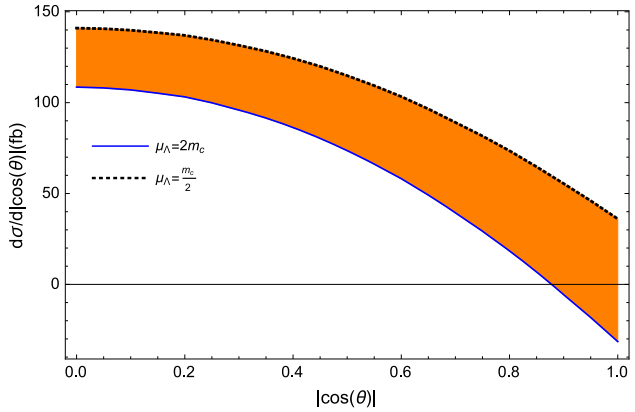

Fig. 7 The angular distribution of η_c production in association with light hadrons at B-factories. The *upper and lower bounds of the band* correspond to $\mu_\Lambda = m_c/2$ and $\mu_\Lambda = 2m_c$, respectively

illustrate the uncertainties brought about by μ_Λ, we present the band corresponding to the range $\frac{m_c}{2} < \mu_\Lambda < 2m_c$ in Fig. 7. One can find that for $\mu_\Lambda = \frac{m_c}{2}$, the differential cross section is already positive in the whole cosθ range.

4 Summary

In this paper, we studied the η_c associated production with light hadrons in e^+e^- collisions at the B-factory energy. This process serves as the best device to test the CO mechanism. We found that the CS contributions are almost negligible, while the ${}^1S_0^{[8]}$ channel dominates the total cross section. The ${}^1P_1^{[8]}$ channel almost vanishes in the total cross section calculation, however, proves to be very important for the angular distribution behaviour. The angular distribution turns out to be downward going when all the CO channels are counted, which is one of the most distinct signal for the CO mechanism. We also studied the μ_r, m_c and μ_Λ dependence. It was found that these dependences are even milder than those for the processes $e^+e^- \to J/\psi + X$ at the same colliding energy. We also presented the first study of the angular distribution of $c\bar{c}({}^1S_0^{[8]})$ production at the B-factories, which might be useful for the understanding of the angular distributions of the J/ψ production measured by Belle.

Acknowledgments This work is supported by the National Natural Science Foundation of China (Nos. 11405268, 10925522, 11021092 and 61190121).

Funded by SCOAP[3].

References

1. K.A. Olive et al., Particle Data Group. Chin. Phys. C. **38**, 090001 (2014)
2. S. Barsuk, J. He, E. Kou, B. Viaud, Phys. Rev. D. **86**, 034011 (2012). arXiv:1202.2273
3. R. Aaij et al., LHCb. Eur. Phys. J. C. **75**, 311 (2015). arXiv:1409.3612
4. G.T. Bodwin, E. Braaten, G.P. Lepage, Phys. Rev. D. **51**, 1125 (1995) (erratum: Phys. Rev. D 55, 5853, 1997). arXiv:hep-ph/9407339
5. S.S. Biswal, K. Sridhar, J. Phys. G. **39**, 015008 (2012). arXiv:1007.5163
6. A.K. Likhoded, A.V. Luchinsky, S.V. Poslavsky, Mod. Phys. Lett. A. **30**, 1550032 (2015). arXiv:1411.1247
7. M. Butenschoen, Z.-G. He, B.A. Kniehl, Phys. Rev. Lett. **114**, 092004 (2015). arXiv:1411.5287
8. H. Han, Y.-Q. Ma, C. Meng, H.-S. Shao, K.-T. Chao, Phys. Rev. Lett. **114**, 092005 (2015). arXiv:1411.7350
9. H.-F. Zhang, Z. Sun, W.-L. Sang, R. Li, Phys. Rev. Lett. **114**, 092006 (2015). arXiv:1412.0508
10. Y.-Q. Ma, K. Wang, K.-T. Chao, Phys. Rev. Lett. **106**, 042002 (2011). arXiv:1009.3655
11. Z. Sun, H.-F. Zhang, arXiv:1505.02675 (2015)
12. L.-K. Hao, F. Yuan, K.-T. Chao, Phys. Rev. Lett. **83**, 4490 (1999). arXiv:hep-ph/9902338
13. L.-K. Hao, F. Yuan, K.-T. Chao, Phys. Rev. D. **62**, 074023 (2000). arXiv:hep-ph/0004203
14. M.E. Biagini et al. (SuperB), arXiv:1009.6178 (2010)
15. T. Abe et al. (Belle-II), arXiv:1011.0352 (2010)
16. M. Butenschoen, B.A. Kniehl, Phys. Rev. D. **84**, 051501 (2011). arXiv:1105.0820
17. K.-T. Chao, Y.-Q. Ma, H.-S. Shao, K. Wang, Y.-J. Zhang, Phys. Rev. Lett. **108**, 242004 (2012). arXiv:1201.2675
18. B. Gong, L.-P. Wan, J.-X. Wang, H.-F. Zhang, Phys. Rev. Lett. **110**, 042002 (2013). arXiv:1205.6682
19. G.T. Bodwin, H.S. Chung, U.-R. Kim, J. Lee, Phys. Rev. Lett. **113**, 022001 (2014). arXiv:1403.3612
20. P. Faccioli, V. Knnz, C. Lourenco, J. Seixas, H.K. Whri, Phys. Lett. B. **736**, 98 (2014). arXiv:1403.3970
21. G.T. Bodwin, K.-T. Chao, H.S. Chung, U.-R. Kim, J. Lee, Y.-Q. Ma, Phys. Rev. D. **93**, 034041 (2016). arXiv:1509.07904
22. B. Aubert et al., (BaBar). Phys. Rev. Lett. **87**, 162002 (2001). arXiv:hep-ex/0106044
23. K. Abe et al., (Belle). Phys. Rev. Lett. **88**, 052001 (2002a). arXiv:hep-ex/0110012
24. K. Abe et al., (Belle). Phys. Rev. Lett. **89**, 142001 (2002b). arXiv:hep-ex/0205104
25. P. Pakhlov et al., (Belle). Phys. Rev. D. **79**, 071101 (2009). arXiv:0901.2775
26. E. Braaten, Y.-Q. Chen, Phys. Rev. Lett. **76**, 730 (1996). doi:10.1103/PhysRevLett.76.730. arXiv:hep-ph/9508373
27. F. Yuan, C.-F. Qiao, K.-T. Chao, Phys. Rev. D. **56**, 321 (1997). arXiv:hep-ph/9703438
28. Y.-J. Zhang, K.-T. Chao, Phys. Rev. Lett. **98**, 092003 (2007). arXiv:hep-ph/0611086
29. Y.-Q. Ma, Y.-J. Zhang, K.-T. Chao, Phys. Rev. Lett. **102**, 162002 (2009). arXiv:0812.5106
30. B. Gong, J.-X. Wang, Phys. Rev. Lett. **102**, 162003 (2009a). arXiv:0901.0117
31. B. Gong, J.-X. Wang, Phys. Rev. D. **80**, 054015 (2009b). arXiv:0904.1103
32. Z.-G. He, Y. Fan, K.-T. Chao, Phys. Rev. D. **81**, 054036 (2010). arXiv:0910.3636

33. Y.-J. Zhang, Y.-Q. Ma, K. Wang, K.-T. Chao, Phys. Rev. D. **81**, 034015 (2010). arXiv:0911.2166
34. H.-S. Shao, JHEP **04**, 182 (2014). arXiv:1402.5840
35. Y.-J. Li, G.-Z. Xu, Y.-J. Zhang, K.-Y. Liu, arXiv:1409.2293 (2014)
36. E.J. Eichten, C. Quigg, Phys. Rev. D. **52**, 1726 (1995). arXiv:hep-ph/9503356
37. M. Beneke, A. Signer, V.A. Smirnov, Phys. Rev. Lett. **80**, 2535 (1998). arXiv:hep-ph/9712302
38. L.-B. Chen, C.-F. Qiao, Phys. Lett. B. **748**, 443 (2015). arXiv:1503.05122
39. F. Feng, Y. Jia, W.-L. Sang, Phys. Rev. Lett. **115**, 222001 (2015). arXiv:1505.02665
40. J.-X. Wang, H.-F. Zhang, Phys. Rev. D. **86**, 074012 (2012). arXiv:1207.2416
41. J.-X. Wang, H.-F. Zhang, J. Phys. G. **42**, 025004 (2015). arXiv:1403.5944
42. H.-F. Zhang, L. Yu, S.-X. Zhang, L. Jia, Phys. Rev. D. **93**, 054033 (2016)(addendum: Phys. Rev. D 93(7), 079901, 2016). arXiv:1410.4032
43. J.-X. Wang, Nucl. Instrum. Methods A **534**, 241 (2004). arXiv:hep-ph/0407058
44. P.L. Cho, A.K. Leibovich, Phys. Rev. D. **53**, 150 (1996). arXiv:hep-ph/9505329